GSA Data Repository Item # 8623

Title of article Reequilibration of Fluid Inclusions in Low-Temperature Calcium Carbonate Cement"

Author(s) Robert H. Goldstein

see Geology **v.** 14 **, p.** 792 **-** 795

Contents 17 pages

Experimental Techniques for Fluid Inclusion Work

ADDITIONAL INFORMATION FOR GEOLOGY PAPER: REEQUILIBRATION OF FLUID INCLUSIONS IN LOW-TEMPERATURE CALCIUM CARBONATE CEMENT

Robert H. Goldstein

University of Wisconsin, Department of Geology and Geophysics, 1215 W. Dayton St., Madison, Wisconsin 53706

Current address: University of Kansas, Department of Geology, Lawrence, Kansas 66045

EXPERIMENTAL TECHNIQUES FOR FLUID INCLUSION WORK

Heating and freezing stages used.:

1) McLimans gas flow heating and freezing stage
2) Reynolds - Fluid Inc. gas flow heating and freezing stage.

Stage Calibration:

1) Calibration for temperatures below 0 °C: Used pure carbon dioxide-water fluid inclusions and identified carbon dioxide melting at -56.6 °C. Attempts to use melting temperatures of various organic solvents failed as their purity was not sufficient for calibration. Attempts to use salt solutions sealed in capillary tubes was judged unsatisfactory as concentration was apparently changed by evaporation during sealing.
2) Calibration for 0 °C: Used thermocouple immersed in distilled water ice bath, melting point of pure water fluid inclusion, melting point of water-filled capillary tube.

3) Calibration above 0 °C: Omega solid melting point standards were used for calibration. Crystals were placed between a piece of glass slide and a cover slip. Small, fluid inclusion size, clumps of crystals were used. Samples were heated rapidly to approach the melting point, were held at a steady temperature for several minutes and then the temperature was increased at a rate of about 0.1 °C per minute until sample had melted.

Sample Preparation:

1) Samples were never heated above room temperature during sample preparation.

2) No samples were stained before fluid inclusion analysis.

3) No samples were studied in cathodoluminescence before fluid inclusion analysis.

4) Some samples were prepared by cleaving crystals with a razor blade and using the cleavage fragments for analysis.

5) Most samples were polished, applied to glass slide using a non-highly exothermic mounting medium wich was allowed to cure at lab temperature. Samples were then cut off thick to prevent heating of the part of the sample near the glass. Samples were then ground down to proper thickness and polished.

6) Polished thin sections were then cut to pieces several millimeters in diameter using a low speed cutoff saw.

Run procedure:

1) Fields of view were mapped and sketched.

2) Thermocouple was positioned close to sample and in contact with chip.

3) Heating runs were done first as freezing runs tended to decrepitate or partially decrepitate the inclusions.

4) Samples were heated rapidly to just below the lowest temperature at which a fluid inclusion in the field of view appeared near homogenization. Samples were stablized and then heated at a rate between 0.5 and 1.0 °C per minute. The lowest Th was recorded first so the measurement recorded is the first time in the lab that the sample had reached its Th. Therefore, overheating was avoided. Heating was continued, noting Th and Td up to a temperature of 250 °C, the temperature at which essentially no phase changes were still observable and the temperature at which the mounting medium turned brown. Several heating runs were repeated to determine repeatability of the measurements and stretching of the inclusions. Most vapor bubbles did not move during the heating runs and therefore the temperature needed to be cycled to attain reliable Th measurements.

5) Samples were cooled to liquid nitrogen temperatures. No changes were observed in the apparently all-gas filled inclusions. In most all-liquid inclusions, no changes were observed, however in some, freezing was detected but data were not attainable because of decrepitation of the inclusions. As warming of frozen inclusions proceeded, rate was slowed at -60 °C and above to observe first melting, intermediate melting and final melting phenomena. All final melting temperatures reported are for those inclusions containing a vapor phase during final melting. Final melting events were cycled to attain valid data and repeated if possible. Many fluid inclusions stretched, partially leaked or totally leaked as a result of the freezing procedure.

SAMPLE DESCRIPTIONS

The following figure, Fig.1, contains descriptions of the samples used, and the contained fluid inclusion populations.

SAMPLE DESCRIPTION			CEMENT DESCRIPTION			FLUID INCLUSION CHARACTERISTICS				
SAMPLE #	OCCURRENCE, SEDIMENTARY UNIT	AGE	CEMENT MINERALOGY	CEMENT FABRICS	INTERPRETED CEMENT ENVIRONMENT	ABUNDANCE	OPTICAL QUALITY	LONG DIMENSION, MICRONS	DISTRIBUTION	APPARENT CONTENT
1	CAVE CALCITE, CARLSBAD CAVERNS, NEW MEXICO	LATE CENOZOIC	CALCITE	FIBROUS-BLADED, BANDED FLOWSTONE	FRESHWATER, VADOSE ZONE	VERY ABUNDANT	GOOD	1.5-70	GROWTH ZONES, CRYSTAL BOUNDARIES	ALL-LIQUID, ALL-GAS, LIQUID-GAS WITH VARIABLE RATIO
2	CAVE CALCITE AND JOINT-FILL, NEVADA	LATE CENOZOIC	CALCITE	EQUANT-FIBROUS, BANDED FLOWSTONE	FRESHWATER, VADOSE ZONE	COMMON	GOOD	3-100	GROWTH ZONES, RANDOM	ALL-LIQUID, ALL-GAS, LIQUID-GAS WITH VARIABLE RATIO
3	EOLIANITE, JOULTERS CAY, BAHAMAS	HOLOCENE	CALCITE	BLADED-EQUANT, MENISCUS AND ISOPACHOUS	FRESHWATER, VADOSE ZONE	COMMON	POOR	5 OR LESS, SOME 15	RANDOM	ALL-LIQUID, ALL-GAS, LIQUID-GAS WITH VARIABLE RATIO
4	LIMESTONE, NEW PROVIDENCE ISLAND, BAHAMAS	PLEISTOCENE	CALCITE	GRANULAR, NO ASYMMETRY	FRESHWATER?, PHREATIC ZONE	RARE-COMMON	POOR	5 OR LESS	RANDOM, CRYSTAL BOUNDARIES	ALL-LIQUID, ALL-GAS, RARE LIQUID-GAS
5	CALOOSAHATCHEE FORMATION, FLORIDA	PLIO-PLEISTOCENE	CALCITE	BLADED-EQUANT, NO ASYMMETRY	FRESHWATER?, PHREATIC ZONE	RARE-COMMON	POOR	8 OR LESS, MOST LESS THAN 3	CRYSTAL BOUNDARIES, RANDOM	ALL-LIQUID, ALL-GAS, RARE LIQUID-GAS
6	MIAMI FORMATION, FLORIDA	PLEISTOCENE	CALCITE	ISOPACHOUS, DOG TOOTH, COARSE BLOCKY, NO ASYMMETRY	FRESHWATER?, PHREATIC ZONE	RARE-COMMON	POOR	10 OR LESS	CRYSTAL BOUNDARIES, RANDOM, GROWTH ZONES	ALL-LIQUID, ALL-GAS, RARE LIQUID-GAS
7	KEY LARGO LIMESTONE, FLORIDA	PLEISTOCENE	CALCITE	COARSE BLOCKY, NO ASYMMETRY	FRESHWATER?, PHREATIC ZONE	RARE	POOR	12 OR LESS	CRYSTAL BOUNDARIES, RANDOM, GROWTH ZONES	ALL-LIQUID, ALL-GAS
8	REEF WALL, OFFSHORE BELIZE	HOLOCENE	ARAGONITE	FIBROUS, BOTRYOIDAL	MARINE, SUBTIDAL	ABUNDANT	POOR	1-200	PARALLEL TO FIBERS, RANDOM	ALL-LIQUID, ALL-GAS, RARE LIQUID-GAS
9	LAKE VALLEY FORMATION, PALEOKARSTIC SURFACE, NEW MEXICO	MISSISSIPPIAN-PENNSYLVANIAN	CALCITE	BLADED-FIBROUS, COMPOSITE CRYSTALS, BANDED FLOWSTONE, PENDANT, MENISCUS	LOW-TEMPERATURE, FRESHWATER, VADOSE-PHREATIC, CAVE OR SURFACE	ABUNDANT	FAIR-GOOD	5-70	GROWTH ZONES, CRYSTAL BOUNDARIES, RANDOM	ALL-LIQUID, ALL-GAS, GAS-LIQUID WITH VARIABLE RATIO
10	LAKE VALLEY FORMATION, NEW MEXICO	MISSISSIPPIAN	CALCITE	SYNTAXIAL OVERGROWTHS ON CRINOID FRAGMENTS	LOW-TEMPERATURE, FRESHWATER, PHREATIC	RARE-COMMON	FAIR	MOST 5, SOME 5-10	WITHIN CRINOID FRAGMENTS, RANDOM, GROWTH ZONES	LIQUID-GAS WITH VARIABLE RATIO, ALL-GAS

BLADED-FIBROUS CALCITE FROM MISSISSIPPIAN-PENNSYLVANIAN KARSTIC SURFACE

In the Sacramento Mountains of New Mexico, Mississippian Strata are unconformably overlain by Pennsylvanian strata. The unconformity surface probably developed from subaerial erosion before the deposition of the Pennsylvanian formations. The surface is marked by solution pockets into the Mississippian limestone and conspicuous channeling at the base of the Pennsylvanian (Pray, 1959).

At one locality, south of High Rolls, New Mexico (see Pray, 1959; p. 49, mi 5.3 for exact location and description), the Mississippian-Pennsylvanian unconformable contact is exposed. Here, the Mississippian Lake Valley Formation consists of crinoidal limestones, the uppermost several meters of which are rubbly and weathered (orange-brown coloration) in appearance. This rubbly zone, which is overlain by Pennsylvanian detrital rocks of the Gobbler Formation, probably represents subaerial alteration of the Lake Valley (Pray, 1959).

The zone of alteration is not well-exposed. In spite of that problem, several interesting features are observable. First, the rubbly nature of the outcrop is distinctive and is composed of rounded "clasts" of Lake Valley Limestone. This feature is very similar to those of Paleokarstic horizons described by Wright (1982) from the Carboniferous of South Wales. Second, large (up to 35 cm wide and at least 50 cm long), irregularly-shaped to channel-shaped voids apparently have been cut into the Lake Valley. These probably were caused by dissolution (karstification) of the Lake Valley. Third, these voids are filled with gray-green and maroon shale. Fourth, the shaly infiltrate is interlayered with coarse masses of bladed calcite spar.

As the first sediment to have filled the solution voids was the gray-green and maroon shale and as that is interlayered with bladed-to-fibrous calcite spar, the calcite most likely precipitated during deposition of the shale. Moreover, as the shale was the first sediment to fill the solution voids (before deposition of the overlying Pennsylvanian Gobbler terrigenous clastics), the whole process of bladed-to-fibrous spar precipitation and shale infiltration must have taken place very early after subaerial void formation. Therefore, the bladed to fibrous calcite spar probably precipitated during the unconformity-producing subaerial exposure event. Thus, the bladed-to-fibrous spar should represent precipitation from surface temperature, meteroic waters and would be a near-surface, cave, spring, or pool deposit.

Numerous hand specimen characteristics support the near-surface interpretation. The extreme coarseness of the calcite crystals is striking. These crystals are as long as 10 cm and as wide as 1.5 cm. The width of individual crystals increases away from the substrate and many samples are finely growth banded and each band is marked by a thin lamina of brownish, iron-oxide-rich clay. Other samples are not finely banded, and the cloudy-white spar is disturbed by a brownish growth band every several cm of crystal length. Crinoid fragments and gray-green, silty clay inclusions rest on growth surfaces within the spar. The bladed-to-fibrous nature of the calcite as well as the fine banding are all supportive of a near-surface origin for the spar. Occurrence of crinoid and silty-clay inclusions are consistent with this interpretation, the silty-clay having been introduced during cement growth and the crinoid fragments (many lacking cement rims) having fallen from the Mississippian host rock.

The environment in which these crystals precipitated can be further refined through petrographic analysis of the samples. The spar is finely growth banded nonferroan calcite. These growth bands are delineated by fluid inclusions and iron oxides, as well as clastic accumulations of calcite crystal fragments, clay, and quartz silt. Some growth bands define coarse, well-developed crystal terminations with as much as 5 mm of relief between the termination and the adjacent trough separating the crystal from its neighbor. In many samples, growth bands define smoothly curved surfaces that are continuous across many crystals and span distances as long as 10 cm. Along these surfaces, coarse, well-developed crystal terminations are rare to absent and most crystals have flat or slightly curved terminations indicative of either erosional truncation of crystal terminations or growth up to a fluid film boundary. Moreover, individual growth zones tend to pinch and swell and whole series of growth zones are, in places, erosionally truncated.

More complex petrographic features are visible on a finer scale, within a single blade or fiber. Many large blades or fibers are composed of tightly-packed, bladed-to-fibrous subcrystals that are all in optical continuity and whose long dimensions parallel that of the larger, master crystal. These subcrystals are approximately 0.1 mm in width and are of variable length. Some of these have steep well-developed terminations, whose faces form angles higher than 45 degrees with the substrate. Therefore, many of these crystals precipitated as length-fast calcite (Dickson, 1978). Other subcrystals within the same master crystal have rounded-to-flat terminations. As these are in optical continuity with the well-terminated crystals and there is no equant, mosaic calcite (indicative of aragonite inversion; Folk and Assereto, 1976), these too were precipitated as length-fast calcite. The flat terminations were either caused by erosion of cement terminations or growth up to some boundary such as a water-air interface (Kendall and Broughton, 1977).

Asymmetric, gravity development of calcite spar is present throughout many of the samples. Both stalactitic and stalagmitic tendencies occur and indicate vadose zone precipitation, however, in some samples and zones, there is no asymmetric cement.

The stable isotopic composition of the spar supports a low-temperature, freshwater, Mississipiian-Pennsylvanian origin for the spar. The average $\delta^{13}C$=-7.3‰ PDB, indicating a large contribution of soil-derived, isotopically light carbon and supporting the near-surface, low-temperature interpretation. The average $\delta^{18}O$=-3.0‰ PDB. This value falls well within the range $\delta^{18}O$ values reported by Meyers et al. (1982) for low-temperature, freshwater calcite precipitation in the Lake Valley Formation. Preservation of these isotopic compositions not only indicates a Mississippian-Pennsylvanian near-surface freshwater origin, but supports the contention that the spar has not recrystallized.

The spar also contains evidence of having been subjected to stress. The calcite is twinned and is cross-cut by fractures filled with ferroan calcite. Moreover, stylolites cross-cut cement fabrics. Therefore, it seems likely that the spar was subjected to considerable burial stress after near-surface precipitation.

In summary, the coarse spar was only found in a horizon recognized as a subaerial unconformity (Pray, 1959) and confirmed as karstic by Meyers (1978). The spar occurs within probable solution pockets and is interbedded with shale that was probably deposited during or shortly after karstification. As crinoid fragments lacking syntaxial rims are present as inclusions in the spar, some spar precipitation must have taken place before complete cementation of the host limestone. This would date the bladed to fibrous spar as pre-Permian (Meyers, 1974, 1978; Meyers et al., 1982). Also, large voids such as the solution pockets observed would have been filled by the overlying

Pennsylvanian sediments if they had not been filled prior to Pennsylvanian deposition. Therefore, the spar must have precipitated close to the timing of the subaerial exposure event. In addition, fine growth banding and inclusions of clastic material suggest the spar grew near a subaerial surface. Asymmetric cement fabrics, truncated crystal terminations, rounded growth surfaces, pinching and swelling of cement zones and erosion of cement zones suggests growth in a vadose environment. Where these fabrics are absent, phreatic growth could have been the norm. The isotopic composition of the spar supports a low-temperature, near-surface, freshwater origin for the spar. Stylolites, twinning and ferroan-calcite filled fractures indicate deep burial after precipitation. Therefore, the spar is most likely a Mississippian-Pennsylvanian speleothem or near surface pool deposit that was subsequently buried beneath the overlying Pennsylvanian, Permian, post-Paleozoic strata, and then later uplifted.

QUANTITATIVE HYDROFRACTURING MODEL

A hydrofracturing model dealing with a spherical inclusion embedded in an infinite isotropic matrix and under confining pressure was published by Van der Molen (1981). The work was developed to consider the case of a quartz inclusion embedded in a granite, but the model can be applied to any general case. Let us examine the case of a spherical, freshwater, all-liquid fluid inclusion that was trapped at 20 ^{o}C and then subjected to burial heating and pressure. The following assumptions must be made:

(1) No plastic deformation. Only brittle deformation occurs. Plastic deformation would tend to decrease the pressure within the fluid inclusion through wall stretching (Bodnar and Bethke, 1984). This would decrease the likelihood that a crack could develop. Such a situation is possible for calcite. However, the evidence of large-scale leakage of fluid inclusions in the cements studied decreases the likelihood that it is the only process acting.

(2) Calcite has strength. To a first approximation it is probably true that calcite has no strength (or very little) along its cleavages. If calcite does have some strength, this would tend to slightly increase the likelihood that fluid inclusions will not fracture their matrix through hydrofracturing.

(3) The inclusion is spherical. Spherical inclusions are rare in nature. Any deviation from that shape would tend to increase the likelihood of a fracture developing. In fact, pointed walls in fluid inclusions would have a wedging effect on the matrix and could greatly increase the possibility of hydrofracturing. The importance of this effect would depend on the shape of the irregularity as well as its orientation with respect to matrix anisotropies.

(4) Calcite and freshwater compressibilities and coefficients of thermal expansion are isotropic. Although freshwater is isotropic, calcite is anisotropic with respect to these properties. Van der Molen argues that this should only have minor effects at first order calculations.

(5) The inclusion is isolated within an infinite matrix. This is certainly not true for a fluid inclusion that is surrounded by other fluid inclusions of various sizes in a tiny, cleaved calcite crystal, which is the case in nature. These perturbations could increase the likelihood of a fluid inclusion hydrofracturing its calcite matrix.

Making the above assumptions, one can calculate a critical geothermal-geopressure gradient above which a low-temperature, freshwater fluid inclusion should not survive. Violation of any of the above assumptions could drive this curve in either direction as described above. Note, this calculation is in a developing stage and will likely evolve as we learn more about the constraints of such systems.

We will use the method and notation of Van der Molen (1981)

σRt is the tangential normal stress at the inclusion surface. If it is less than 0, stress is tensional and a crack will develop normal to the inclusion surface.

A is the volumetric thermal expansion coefficient.

T is the temperature in ^{o}C.

P is the external pressure in kilobars.

P' is the fluid inclusion internal pressure in kilobars.

u is the aggregate shear modulus of calcite.

K is the aggregate bulk modulus of calcite.

K' is the bulk modulus of water.

(1) $\sigma Rt \leq 0$ when $- \Delta T \, \Delta A \geq P \, (3/2u + 3/K' - 1/K)$

Likewise, if one assumes the isochore pressures to be real and assumes some geothermal gradient, the tangential stress at the inclusion surface can be calculated at a given temperature using the relationship:

(2) $Rt = 3/2\ P - 1/2\ P'$

The critical geothermal-geopressure gradient calculated by relationship (1) using data of Burnham et al., (1969), Simmons and Wang, (1971), Skinner, (1966), and Keenan et al., (1978), shows that if a fluid inclusion were trapped as all-liquid, freshwater and buried from 20 ^{o}C through the hydrostatic geothermal-geopressure gradient diagrammed (about 1.1 ^{o}C/100 feet and 3.1 bars/100 feet), the fluid inclusion would begin hydrofracturing and leaking at about 30 ^{o}C and would continue to do so with continued burial (Fig. 2). If the same fluid inclusion were buried through the lithostatic geopressure-geothermal gradient diagrammed (an unlikely possibility at about 1.1 ^{o}C/100 feet and 6.9 bars/100 feet), fluid inclusions would start causing fractures and leaking at a depth where a geothermal temperature of about 130 ^{o}C would be reached. In the diagenetic realm, pressures would most likely approximate some gradient between the lithostatic and hydrostatic line (possibly 2/3 lithostatic). Thus, early primary fluid inclusions would hydrofracture their calcite matrices and leak in most burial environments deeper than about 3 km. Fluid inclusions buried to depths of 3 km or less may or may not survive, depending upon the geothermal-geopressure gradient and the degree to which the stated assumptions are violated for each fluid inclusion.

A relationship calculated from equation (2) gives similar results. If one compares the isochore pressure within the inclusion to the same hydrostatic, geopressure-geothermal gradient used above, one finds that freshwater fluid inclusions trapped at low-temperature and subsequently buried, would begin hydrofracturing at about 50 ^{o}C, and could continue

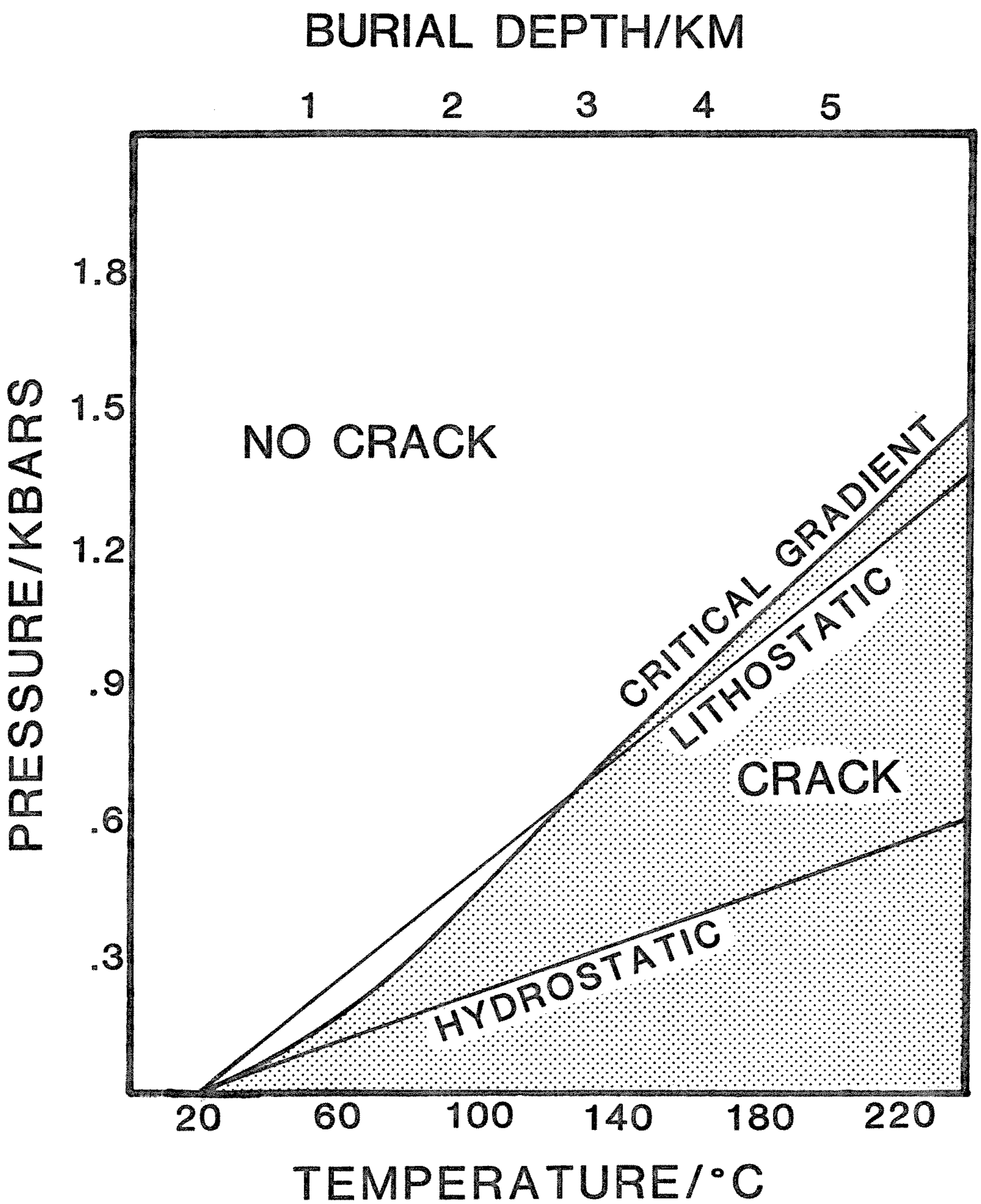
BURIAL DEPTH/KM
1
2
3
4
5
1.8
1.5
1.2
.9
.6
.3
PRESSURE/KBARS
NO CRACK
CRITICAL GRADIENT
LITHOSTATIC
CRACK
HYDROSTATIC
20
60
100
140
180
220
TEMPERATURE/°C

RHG '84

cracking during burial. This result is in close agreement with that obtained by equation (1). If one assumes the lithostatic gradient, it appears that external pressure would be high enough throughout deep-burial diagenetic conditions to prevent hydrofracturing. As this gradient is unusual, hydrofracturing probably does occur. The different results obtained by the two methods can be explained by the unreal assumption that the fluid inclusion isochores used with equation (2) actually represent pressures within the inclusion.

These calculations show the extreme likelihood of low-temperature fluid inclusions hydrofracturing when they are buried through a hydrostatic, geothermal-geopressure gradient. At some combination of lithostatic and hydrostatic, the critical curve may straddle the gradient and fluid inclusions may or may not hydrofracture down to a maximum burial depth of about 3 km. At lithostatic geopressure, fluid inclusions will not hydrofracture or will at least only hydrofracture when they reach depths sufficiently high to have raised ambient temperature to greater than 130 ^{o}C. If assumptions (1) and (2) were violated, then more fluid inclusions would survive without hydrofracturing. Violation of assumptions (3) and (5) would tend to greatly increase the ease of hydrofracturing of fluid inclusions.

REFERENCES CITED

Bodnar, R.J., and Bethke, P.M., 1984, Systematics of stretching of fluid inclusions I: Fluorite and sphalerite at 1 atmosphere confining pressure: Economic Geology, v. 79, p. 141-161.

Burnham, W.C., Holloway, J.R., and Davis, N.F., 1969, Thermodynamic properties of water at 1,000 9C and 10,000 bars: Geological Society of America Special Paper 132, 96 p.

Dickson, J.A.D., 1978, Length-slow and length-fast calcite: A tale of two elongations: Geology, v. 6, p. 560-561.

Folk, R.L., and Assereto, Riccardo, 1976, Comparative fabrics of length-slow and length-fast calcite and calcitized aragonite in a Holocene speleothem, Carlsbad Caverns, New Mexico: Journal of Sedimentary Petrology, v. 46, p. 486-496.

Keenan, J.H., Keyse, F.G., Hill, P.G., and Moore, J.G., 1978, Steam tables: New York, John Wiley and Sons, 136 p.

Kendall, A.C., and Broughton, P.L., 1977, 'Discussion of Calcite and aragonite fabrics, Carlsbad Caverns': Journal of Sedimentary Petrology, v. 47, p. 1397-1400.

Meyers, W.J., 1974, Carbonate cement stratigraphy for the Mississippian Lake Valley Formation, Sacramento Mountains, New Mexico: Journal of Sedimentary Petrology, v. 44, p. 1078-1088.

Meyers, W.J., 1978, Carbonate cements: Their regional distribution and interpretation in Mississippian limestones of southwestern New Mexico: Sedimentology, v. 25, p. 371-400.

Meyers, W.J., Cowan, P. and Lohman, K.C., 1982, Diagenesis of Mississippian skeletal limestones and bioherm muds, New Mexico, in Bolton, K, Lane, H.R., and LeMone, D.V. eds., Symposium on the paleoenvironmental setting and distribution of the Waulsortian Facies: El Paso Geological Society and University of Texas, El Paso, p. 80-95.

Pray, L.C., 1959, Sacramento Mountains of Otero County, New Mexico: Society of Economic Paleontologists and Mineralogists, Permian Basin Section and Roswell Geological Society Guidebook for joint field conference, 306 p.

Simmons, Gene, and Wang, Herbert, 1971, Single crystal elastic constants and calculated aggregate properties: A handbook: Cambridge, M.I.T. Press, 370 p.

Skinner, B.J., 1966, Thermal expansion, in Clark, ed., Handbook of physical constants: Geological Society of America Memoir 97, p. 75-96.

Van der Molen, I., 1981, The shift of the alpha-beta transition temperature of quartz associated with the thermal expansion of granite at high pressure: Tectonophysics, v. 73, p. 323-342.

Wright, V.P., 1982, The recognition and interpretation of paleokarsts: Two examples from the Lower Carboniferous of South Wales: Journal of Sedimentary Petrology, v. 52, p. 83-94.